Review

Not peer-reviewed version

Neutron Capture in Evolved Red Giants: A Review

Maurizio Maria Busso *

Posted Date: 28 April 2026

doi: 10.20944/preprints202604.1933.v1

Keywords: stars; evolution of stars; low and intermediate mass; nucleosynthesis

Review

Neutron Capture in Evolved Red Giants: A Review

Maurizio Maria Busso [1,2]

[1] Department of Physics and Geology, Univrsity of Perugia, Perugia, Italy; maurizio.busso@unipg.it or bussom@infn.it
[2] Istituto Nazionale di Fisica Nucleare, Section of Perugia, Perugia, Italy

Abstract

This review traces how our understanding of Low and Intermediate Mass Stars (hereafter LMS and IMS, respectively) evolved in time, in parallel with our knowledge of slow neutron-capture phenomena (the *s*-process). I shall focus in particular on the *main component* of this nucleosynthesis phenomenon, occurring in the above mentioned stars close to the end of their lifetimes. At that stage, they ascend the Asymptotic Giant Branch (AGB), where both hydrogen and helium shells exist, burning alternatively during the phases most relevant to our discussion (the so-called *TP-AGB* phases). I shall outline how neutron sources were discovered to be activated there and what observational constraints and nuclear measurements have taught us about the status of our theoretical models in this field of nuclear and stellar physics research.

Keywords: stars; evolution of stars; low and intermediate mass; nucleosynthesis

---

1. Introduction

The most abundant nuclei, those dominating the solar composition, are produced by fusion reactions, which at the same time supply the energy that fuels stellar evolution. The earliest exploration of these processes, in the 1950's, founded the field now known as *nuclear astrophysics*.

This story actually began much earlier, perhaps at the invention of the mass spectrometer by the British chemist Francis William Aston (Nobel Prize for Physics in 1922) [1]. He discovered that a helium nucleus weighs less than four separate protons, implying that the mass excess could be transformed into energy. This observation prompted Eddington [2] and Perrin [3], independently, to propose that the Sun's luminosity would arise from hydrogen fusion, the resulting mass deficit being released as radiation.

Subsequent investigations by [4,5] about the Coulomb barrier and the tunneling effect required to surmount it were fundamental for the first practical suggestions on how nuclear fusion could occur at the solar temperature [6–8]. Over these foundations, Fred Hoyle later constructed his comprehensive theory of stellar nucleosynthesis [9,10].

1.1. The Way to Neutron Captures

For nuclei heavier than the iron group, the average binding energy decreases with atomic mass. Because of this, producing the heaviest nuclides via the same fusion chains that operate for lighter elements is impossible: those reactions would actually become endothermic and would also need unrealistically high temperatures to overcome the large Coulomb barriers.

Until the fifties, ^{56}Fe was thought to possess the maximum nuclear binding energy B, but works by [11] later showed that the highest value was actually owned by ^{62}Ni, closely followed by the stable ^{58}Fe nucleus. Beyond nickel, the downward slope of the binding energy curve implies that processes different than thermonuclear fusion of charged nuclei must be at work.

The landmark paper by E.M. Burbidge et al. (1957) [12] (later known by the shorthand B^{2}FH) showed that the very heavy elements from Fe to actinides originate mainly through neutron capture reactions. Two limiting regimes were defined:

- r-process (rapid captures, on average faster than β decays along the nuclear path)
- s-process (slow captures, on average slower than β decays along the nuclear path)

At the start of the 1960's, Donald Clayton and co-workers undertook the first quantitative treatment of these capture chains [13,14]. Their analysis (the celebrated CFHZ paper) provided a solution to a simplified s-process equation, based on an exponential distribution of neutron exposures (see later, eq. (4)).

1.2. Early Theoretical Developments

The idea advanced by [13] and [14]. inspired a sequence of follow-up studies that validated and extended it, culminating in the synthesis paper by Seeger et al. [15]. This work produced a complete description of neutron capture nucleosynthesis, fitting the solar σ N curve for "s only" isotopes (those formed solely through the s process), adopting a model based on the already mentioned exponential distribution of neutron exposures and showing that the predicted σN_s curve also reproduced the s-component of solar isotopes with a mixed origin. These findings, illustrated in detail in Clayton's classic textbook [16], remains a cornerstone of this field.

In examining the alternative reaction paths through strontium or rubidium isotopes, Seeger et al. also introduced a first discussion of branching reactions, occurring at the locations along the s-process trajectory where β decay and neutron capture would proceed at comparable rates, splitting the nucleosynthetic flow.

1.3. From Phenomenology to Stellar Models

Near the end of the 1960's, quantitative stellar calculations had begun to appear. The discovery, at the surfaces of red giants (type S), of the unstable element technetium (Tc), with a number of protons $Z = 43$ and lifetimes of its isotopes all much shorter than the stellar evolutionary lifetime [17], demonstrated that slow neutron captures do indeed operate within such evolved stars.

Early attempts to simulate the complex structure of these objects, especially in the work by Schwarzschild & Härm [18], revealed that their energy production arises from two burning shells (of hydrogen and helium) prone to recurrent instabilities, later called *thermal pulses* (TP). The corresponding evolutionary phase thus became known as the *Thermally Pulsing Asymptotic Giant Branch* $(TP-AGB)$ stage.

In the following sections I shall trace, more or less in chronological order, how the field progressed from phenomenological treatments to the first self consistent AGB evolutionary models, beginning with the deductions drawn purely from nuclear systematics.

2. The Phenomenological Approach

As mentioned earlier, the first formal mathematical framework describing the s process was introduced by [13] and by [15], That treatment, now customarily called the *phenomenological approach*, applied elementary nuclear reasoning to reproduce the chain of slow neutron captures that links adjacent stable nuclei. They consider sequential neutron captures on two stable nuclei with atomic masses $(A-1)$ and (A). In their treatment, the time variation of the abundance $N(A)$ of the heavier isotope can be written as:

$$\frac{dN(A)}{dt} = N(A-1)n_n < \sigma_{(A-1)}v > -N(A)n_n < \sigma_{(A)}v > \quad (1)$$

where the brackets indicate the Maxwellian averaged product of cross section and particle velocity and n_n is the neutron density.

In order to quantify the cumulative neutron fluence, one then defines the integrated *neutron exposure*, τ, as:

$$\tau = \int_0^t n_n v_T dt \quad (2)$$

where v_T in the thermal velocity and the integral is extended over the duration t of the exposure. When a system reaches a steady state of continuous neutron flow ($dN/d\tau = 0$), then the previous expression yields the simple relation:

$$< \sigma v >= const. \tag{3}$$

Thus, under equilibrium s processing, the product σN should stay roughly constant for neighbouring isotopes.

The above empirical rule is indeed verified (at least approximately) for the nuclei in the solar system deriving from slow neutron captures, except near nuclear regions of exceptional stability, as predicted by the shell model of the nucleus, where in fact the closure of neutron shells produces abrupt changes in nuclear size and exceptionally low capture cross sections.

Such regions of stability are characterized by specific numbers of neutrons (called *magic neutron numbers*; they are N = 2, 8, 20, 28, 50, 82, 126) and mark discontinuities in the σN distribution. Isotopes possessing these numbers appear also as abundance peaks: they are abundant because their cross sections are much smaller (only a few millibarns) than in adjacent plateaus.

To reproduce the observed solar σN pattern, [15] noted that a distribution of neutron exposures should have contributed (rather than a single value). Any function decreasing with increasing exposure τ might in principle fit the data. The above authors adopted a simple exponential representation:

$$\varrho(\tau) = \frac{GN_{\odot}^{56}}{\tau_0} e^{-\frac{\tau}{\tau_0}} \tag{4}$$

where G is the fraction of the solar $N_{\odot}^{56}$ exposed to neutron fluences and τ_0 is a free parameter (called the *mean* neutron exposure). The value must be chosen that best reproduces the known products of cross sections and solar abundances.

Building on the above assumptions, Clayton and Ward [19] derived an explicit analytical solution for the s process abundance fractions $N_s(A)$) of the solar abundances:

$$\sigma(A)N(A) = \frac{GN_{\odot}^{56}}{\tau_0} \prod_{i=56}^{A} (1 + \frac{1}{\sigma_i \tau_0})^{-1} \tag{5}$$

As it became clear that a single exposure distribution could not circumvent the "bottlenecks" created by magic nuclei, the data were better reproduced by three combined components, each characterized by its own τ_0:

- *Weak* component, responsible for nuclides up to Sr ($N \lesssim 50$);
- *Main* component, for species between Sr and Pb ($50 \lesssim N \lesssim 126$);
- *Strong* component, required mainly to account for the doubly magic ^{208}Pb.

Today, it is recognized that the weak component has to be ascribed to massive stars ($M \gtrsim 10M_{\odot}$) in their phases of combustion of He and C [20], while the rest is mostly due to lower mass stars ($M \lesssim 4M_{\odot}$) of different metallicities, in their TP-AGB stage. [21].

Following earlier hints by [15], a full theoretical treatment of branching point positions along the capture chain, where β decays compete with neutron captures, was provided by [22]. Abundances around such branchings allow one to estimate the physical conditions at the site of nucleosynthesis (neutron density n_n and temperature, T), via a branching ratio (f_-):

$$f_- = \frac{\lambda(\beta_-)}{\lambda(\beta_-) + \lambda_n} \tag{6}$$

where $\lambda(\beta_-) = 1/\tau_{\beta\_}$ is the β decay rate, $\lambda_n = n_n\langle\sigma v\rangle$ is the neutron capture rate.

Since many β-decay rates vary with temperature, the combination of nuclear data and the four parameters G, τ_0, n_n, and T offered practical diagnostics for comparing theoretical conditions with stellar observations.

These quantities acted as the first bridge between pure nuclear physics and astrophysical modeling, guiding later efforts to identify the actual stellar environments where the s process takes place. These will be discussed in section 3

3. Nucleosynthesis Models for AGB Stars

Soon after [15] proposed exponential distributions of neutron exposures, stellar evolution models were extended to the late phases of low and intermediate mass stars. It quickly became clear that the AGB stage, powered simultaneously by hydrogen and helium burning shells, has a distinct behaviour, which strongly affects s-process nucleosynthesis.

3.1. The Thin Shell Instability

In a seminal work, Schwarzschild and Härm [18] identified the mentioned key feature in what they called the *thin shell instability*. Consider, in spherical symmetry, a shell of constant mass (Δm) located at radius r with a small thickness $l(r)$, so that $\Delta m \simeq 4\pi\rho r^2 \times l$. For such a configuration, in hydrostatic equilibrium:

$$\frac{dP}{P} = -4\frac{dr}{r} \tag{7}$$

and consequently;

$$\frac{d\rho}{\rho} = -\frac{dl}{l} \simeq -\frac{dr}{l} = -\frac{rdr}{lr}, \tag{8}$$

which leads to

$$\frac{dP}{P} = 4\frac{ld\rho}{l\rho} \tag{9}$$

Within a stellar plasma an equation of state holds:

$$\frac{dP}{P} = \alpha\frac{dr}{r} + \beta\frac{dT}{T} \tag{10}$$

So that, finally:

$$4(\frac{l}{r} - \alpha)\frac{d\rho}{\rho} = \beta\frac{dT}{T} \tag{11}$$

However, for thermal stability one would require:

$$4\frac{l}{r} < \alpha \tag{12}$$

that, for very thin shells (l/r –> 0) is not always satisfied, creating an unstable situation.

If the shell expands and the hydrostatic pressure falls faster with radius than it would decrease due to the expansion, the layer continues to expand and cool, departing from equilibrium. If instead the temperature rises, a thermonuclear runaway occurs, sharply increasing luminosity before the system relaxes again. See e.g. [23] for a discussion.

3.2. The Double Shell Structure and the Thermal Pulses

Repeated instabilities of the kind mentioned above shape the last stages of evolution in AGB stars. As an example, in models of a $3M_\odot$ star, the luminosity of the He shell shows recurrent sharp peaks up to almost $10^7 L_\odot$, while the H-shell luminosity declines (see Figure 1).

Each episode, known as a thermal pulse (TP), creates a convective zone extending over most of the inter-shell structure, whose initial composition is dominate by He, left behind by shell H burning. As these events recur, helium burns above the core, made of C and O, which is characterized by a degenerate structure (a quantum Fermi gas). This burning is very peculiar; the star experiences sudden He *flashes*, separated by quiescent intervals where H burning dominates the energy production (see again Figure 1). When helium burning ignites (after accumulating enough fuel during the preceding

 doi:10.20944/preprints202604.1933.v1

quiescent phase), the local temperature surges from $\simeq 1.5 \times 10^8$K up to 2.8 - 3.5×10^8K, the exact value depending mainly on the stellar mass.

The enormous energy release from a thermal pulse triggers an intermediate convective zone (*ICZ*) that mixes the products of He burning (including carbon and neutron-capture nuclei) throughout the inter-shell region. In the following expansion and cooling, hydrogen burning stops temporarily, and in the phase that follows, the convective envelope penetrates inward, crossing the H–He discontinuity. This is the so-called *Third Dredge Up* (TDU) phenomenon, carrying He-burning ashes, especially newly created carbon and *s*-elements, to the surface. (This is illustrated schematically in the cartoon of Figure 2).

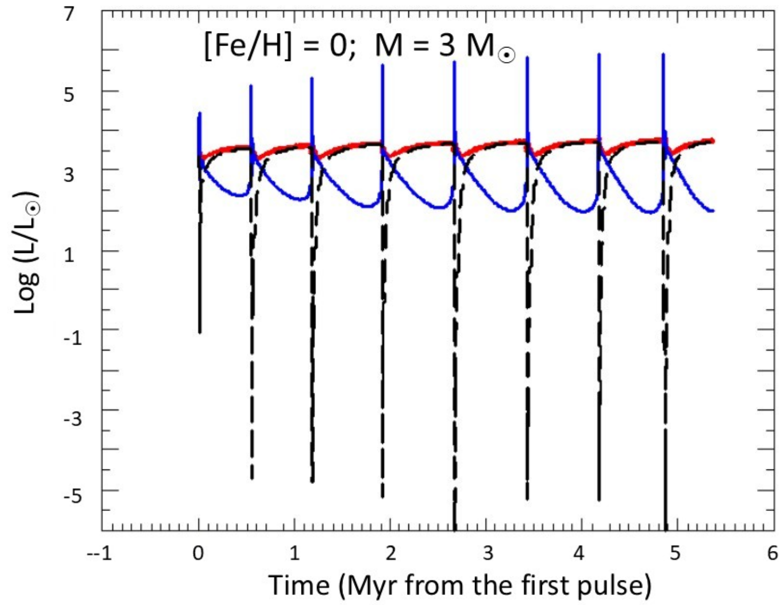

Figure 1. The variation of the luminosity from H-shell and He-shell burning in a modern model of a 3 $M_\odot$ AGB star, Note the peaks in correspondance of He-shell flashes (taken, with modifications, from Halabi [24]).

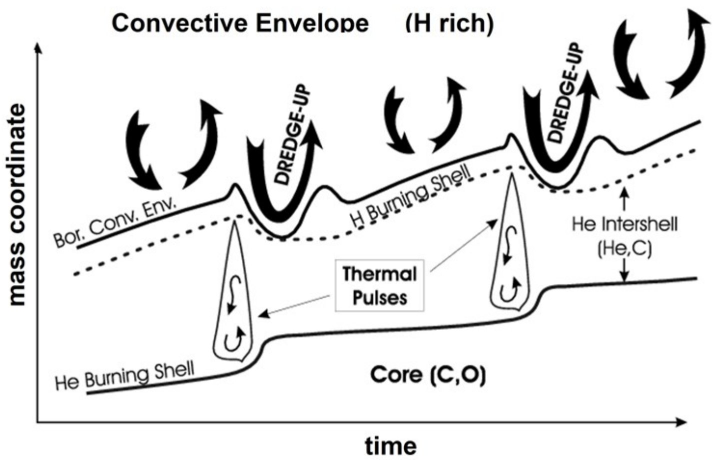

Figure 2. A schematic view of the internal structure of the two-shell region in an AGB star, experiencing thermal pulses, ICZs creation and the third dredge-up. The plot was made by the author and originally published in [21].

Preprints.org (www.preprints.org) | NOT PEER-REVIEWED | Posted: 28 April 2026 doi:10.20944/preprints202604.1933.v1

Despite the occurrence of dredge up, the large envelope mass prevents stars on mass larger thatn 4-5 $M_\odot$ to become C rich at the point that C dominates the photosphere composition and the formation of C-based molecules. These more massive stars and the efforts made to obtain from them a full description of the *s* process will be addrssed in section 4.1.

For stars in the mass range 1.5 to 3 - 4 $M_\odot$, instead, the TDU can raise the C/O ratio above unity, producing the so-called carbon stars [21]. At the base of each *ICZ*, temperatures between 2.8×10^8 and 3.5×10^8K enable several α captures to occur. Apart from the 3 α process, α captures occur mainly on the abundant ^{14}N, left behind by the CNO cycle. This initiates the reaction chain:

$$^{14}N(\alpha,\gamma)^{18}F(\beta^+\nu)^{18}O(\alpha,\gamma)^{22}Ne \tag{13}$$

While the luminosìty undergoes the mentioned variations, the position in mass of the layers where H and He are burning and of the bottom edge of the convective envelope vary accordingly in a rather peculiar manner, changing sharply the behavior previously displayed after the end of core He-burning. The whole evolution of the internal structure during the second ascent to the RGB branch for a 3 $M_\odot$ stellar model of 1/3 solar metallicity, computed with the FRANEC (Fasacati Raphson-Newton Evolutionary Code, see e.g. [25]), is shown in Figure 3. Two different stages of evolution are clearly visible, and are currently referred to as *early-AGB* stage (the first part of figure 3, at the left of the continuous vertical red line), where the H shell is almost extinguished and the He shell grows in mass producing the bulk of the energy) and the already mentioned *TP-AGB* phase (the second part of Figure 3, on the right side of the plot, with the stepwise growth of the He shell in correspondence with the shell flashes).

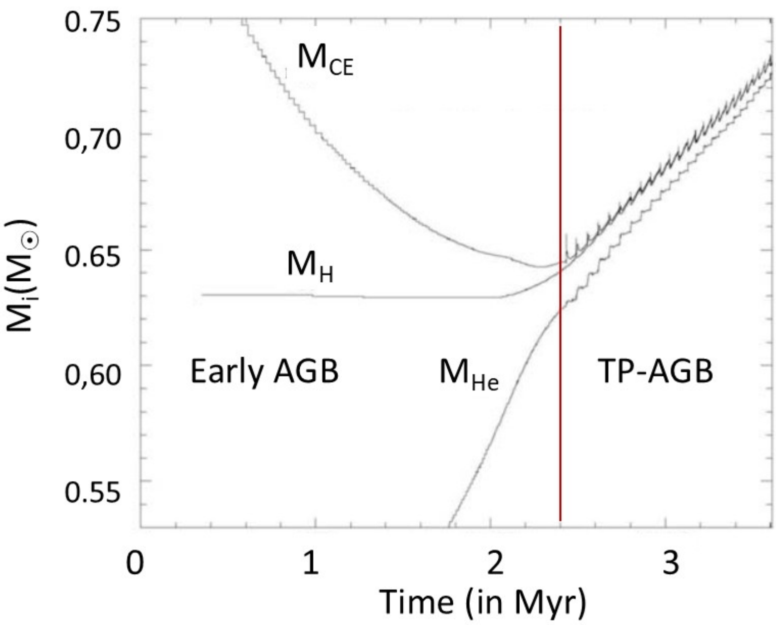

Figure 3. The plot shows the evolution in mass of the layers where He-burning, H-burning and the bottom on the convective envelope are sited, for a star of 3.0 $M_\odot$ and a metallicity of one third solar. At the left of the red continuous vertical line is the early-AGB stage, at the right of it the TP-AGB phase, near the end of which the envelope penetrates below the H-He discontinuity, bringing to the surface C and *s*-elements.

4. The Long Search for a Suitable Neutron Source

The series of reactions (13), when the temperature at the base of the ICZs becomes $T \gtrsim 2.8 \times 10^8$K, can be followed by the two alternative processes:

$$^{22}\mathrm{Ne}(\alpha,\gamma)^{26}\mathrm{Mg}, \tag{14}$$

and

$$^{22}\mathrm{Ne}(\alpha,\mathrm{n})^{25}\mathrm{Mg}, \tag{15}$$

At around 300MK, the ratio of reaction rates $\langle\sigma v\rangle(\alpha,n)$ / $\langle\sigma v\rangle(\alpha,\gamma)$ is close to 3, making reaction (15) the dominant channel and releasing neutrons in the plasma. For roughly two decades, this process, occurring naturally for sufficiently high values of the temperature, was therefore assumed to be at the origin of slow neutron captures in AGB stars, accounting for the detection of technetium [17], whose isotope ^{99}Tc lays directly on the foreseen path of neutron captures and beta decays for the s process.

4.1. The Research on the ^{22}Ne Source Activation

The above interpretation received an apparent confirmation from [26], who showed how an exponentially decreasing distributions of neutron exposures (as proposed by [15]) could arise directly by a series of helium shell flashes.

The properties of TP-AGB stars undergoing the thin shell instabilities discussed so far were investigated analytically by[27,28] in the early 1970s. In this way, relations connecting basic evolutionary quantities (such as the interpulse period, the total luminosity, the advancement rate of the hydrogen burning shell) to the hydrogen exhausted core mass M_H were established. Because the thermal pulse properties depend mainly on such a core mass, different evolutionary models agree in showing a convergence toward a narrow range of parameters. This convergence reflects the common structure of low and intermediate mass stars: a thin active layer sitting above a degenerate C–O core of mass below the Chandrasekhar limit.

The phenomenonn of the third dredge up is more easily found at low metallicities, at least for the stars of mass lower than 2 $M_\odot$. An example of this is shown in Figure 4, again taken from the outputs of the FRANEC code and representing a star of 1.5 $M_\odot$ and a metallity of 1/20th that of the Sun. After every thermal pulse, the envelope penetrates deeper (the TDU), while the H burning shell advances outward. Outside there is the huge convective envelope, with a photospheric temperature quite low for stars ($T \lesssim 3500$ K). The envelope loses mass at increasing rates, through radiation pressure exerted on circumstellar dust grains.

Until the end of the XXth century computing a full evolutionary sequence for a relatively low mass star, with dredge up and nucleosynthesis, was extremely time consuming, so that semi-analytical models became rather popular. They could provide a workable approximation to the real TP-AGB behaviour and useful yield estimates, with a larger efficiency than by running full stellar models. As examples of these approaches see e.g. [29–31]. During the seventies and the eighties AGBs were assumed to have the structure illustrated above up to 7-8 $M_\odot$. As the neutron source shown in relation (15) requires rather high temperature ($T \simeq 3.3 - 3.5 \times 10^8$ K), which is experienced only by stars above about at least 4 $M_\odot$ (i.e. the so-called *Intermediate Mass Stars*, or IMSs) most theoretical work dedicated to study the Main Component of s processing ($88 \lesssim A \lesssim 208$) were concentrated on IMSs and on specifying the rate of what became commonly known as the ^{22}*Ne neutron source*. In these studies a role of particular importance was gained by the groups in Urbana and Chicago, lead by Icko Iben and Jim Truran (see e.g. [32–35]).

A problem however arose when AGB stars enriched in s process elements were shown observationally to be low mass objects, conflicting with the high temperatures required for the $^{22}\mathrm{Ne}(\alpha,n)$ source.

The above fact was pointed out especially by David Lambert and his coworkers (see e.g. [36–38]. Icko Iben [39] early recognized the discrepancy and, with A. Renzini [40], proposed that the neutron production could instead originate from the alternative reaction $^{13}\mathrm{C}(\alpha,n)^{16}\mathrm{O}$ source, operating at a low temperature ($T \gtrsim 8 - 9 \times 10^7$ K). This idea initiated a new line of inquiry, that would dominate subsequent research.

 doi:10.20944/preprints202604.1933.v1

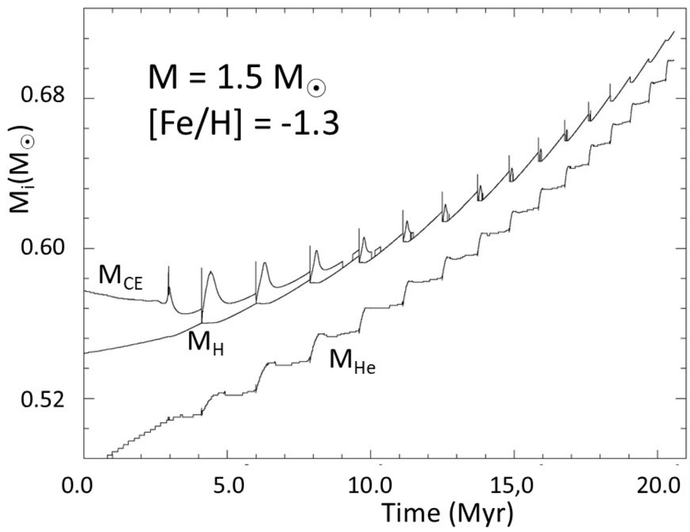

Figure 4. The position in mass of the convective envelope bottom ($M : CE$), of the H-exhausted core (M_H) and of the He-exhausted core (M_He) in a 1.5 $M_\odot$ model star with a metallicity 1/20th solar (Here, as usual, $[Fe/H] = Log(Fe/H)_* - Log(Fe/H)_\odot$. Even for such a low mass, the low metallicity permits the occurrence of the TDU.

4.2. Emergence of the ^{13}C Neutron Source

During the interpulse phase, the reaction $^{13}C(\alpha, n)^{16}O$ becomes active in the inter shell region because, as mentioned, it requires a relatively low temperature to occur. However, the small amount of ^{13}C left behind by shell-H burning is largely insufficient to promote any noticeable neutron flux, also because it comes with a dominant concentration of ^{14}N, which is an efficient neutron absorber. Hence in normal conditions only a marginal number of the Fe nuclei would experience neutron captures and this was the main reason why the neutron production from α captures on ^{13}C was not considered of importance for about thirty years after the work by [13] and [15], mentioned in section 2. In fact, obtaining abundant ^{13}C requires special mixing phenomena to add protons into the He layers, something not generally considered in standard stellar evolution codes.

At the end of the 1980s, however, the existence of similar *extra mixing* processes had been shown to be needed, starting from the RGB phase, by several observational works, indicating especially anomalous carbon isotopic ratios and Li abundances [41–43].

A large spectroscopic evidence also accumulated for the surface enrichment of *s* process elements in AGB stars (of spectral types MS, S, SC, and C(N)). Most of them pointed to low masses for the parent stars.

The above findings also strengthened the conclusion that repeated dredge up events during the TP-AGB phase were at the origin of the appearance at the surface of heavy elements synthesized in the interior [23,44,45]. It became soon indisputable that *s*-element rich AGB stars were low mass objects, meaning that their neutron production could not result primarily from the ^{22}Ne source, whose activation requires, as mentioned, quite high temperatures.

A few years after the early suggestions by Iben and Renzini [40], the research group directed by R. Gallino in Torino verified the inadequacy of ^{22}Ne as a neutron source, indicating that it would have provided both an insufficient exposure and an excessive neutron density, incompatible with solar abundance ratios near the neutron magic nuclei [46]. Soon after, this group demonstrated, with detailed network calculations [47], that neutron fluxes provided by the ^{13}C neutron source were instead potentially suitable to satisfy these two fundamental constraints. This suggestion was carefully controlled and cobfirmed later by [48], with a detailed analysis of reaction branchings along the *s* process path.

 doi:10.20944/preprints202604.1933.v1

4.3. Some Details on How the New Neutron Source Is Activated

In TP-AGB stars, the repeated mixing of the outer convection zone into deeper layers (the already mentioned TDU) not only carries processed material to the surface, but also sets the stage for the main *s*-process neutron source. During a TDU event, the hydrogen rich convective envelope momentarily reaches down into the He and C rich intershell region left by He shell burning. At this moment, the hydrogen burning shell is dormant, so if a small number of protons diffuses into the adjacent zone where ^{12}C is abundant, these protons undergo the capture reactions:

$$^{12}\mathrm{C}(p,\gamma)^{13}\mathrm{N}$$

followed by the inverse β decay of ^{13}N into ^{13}C. The result is a thin layer, in the He-rich zone, with enhanced ^{13}C, just below the envelope. This localized enhancement of ^{13}C (sometimes called the ^{13}C pocket) becomes crucial because, during the long quiescent period between thermal pulses, temperatures overcomes $7-9\times10^7$ K and the reaction:

$$^{13}\mathrm{C}(\alpha,n)^{16}\mathrm{O}$$

begins releasing free neutrons [49,50]. This supply of neutrons under radiative conditions at relatively low neutron density provides the bulk of the neutron exposure that builds heavy elements via slow neutron captures in low mass AGB stars.

Exactly how that pocket forms is still a debated open question, although specific models for that have already been presented, with very encouraging quantitative results [51].

The simplest ingredient is the behavior of convection near the H-He interface. During TDU, when the convective envelope intrudes into the hydrogen exhausted region, there is a steep drop in hydrogen abundance, causing a sharp change in the opacity and temperature gradient. In this situation the exact boundary between convective and stable layers becomes blurred, and even small overshoot of material beyond the formal convective border can mix protons into the radiative zone. Stellar models that include a smoothly declining convective velocity beyond the Schwarzschild boundary naturally produce a gradual hydrogen profile. After TDU, as hydrogen burning resumes, this gradient allows just enough proton captures on ^{12}C to build up ^{13}C in a thin transition layer. Under favorable conditions, this layer can contain $\simeq 10^{-5}$ to $10^{-4}M_\odot$ of ^{13}C, i.e. enough fuel to produce the neutron fluence needed for the main *s* process component.

Beyond this basic convective overshoot picture, more effective physical processes have been proposed to contribute to the required mixing. Two seem prsently most promising:

- Internal gravity waves: Convective turbulence at the base of the envelope generates gravity waves that propagate into the stable layers. Under certain conditions these waves can induce shear and turbulence that transport protons downward during TDU. This gravity wave–induced mixing offers a physically plausible way to naturally seed the ^{13}C pocket without relying purely on ad-hoc overshoot prescriptions [52,53].
- Magnetic mixing: Observations and theoretical studies now indicate that magnetic fields, buried in the deep convective envelope, can produce buoyancy-driven motions and circulation patterns at the H-He interface. Magneto-hydrodynamic (MHD) effects can drive sustained mixing of proton-rich material into the underlying radiative region during TDU, leading to the formation of rather large ^{13}C reservoirs with very low (if any) ^{14}N abundances (see e.g, [51,54] for detailed MHD models in this scenario). This kind of magnetic mixing induces the formation of ^{13}C pockets with a distinguished abundance pattern (see Figure 5) and their repetiton at every pulse has been successfully shown to be able to explain the heavy element enrichment in AGB stars and in post-AGB sources, as well as to interpret various isotopic patterns in stellar ejecta and pre-solar grains [55–58]. It also provided the most accurate separation so far available of the *s* and *r* components in the solar distribution [59]. For this last test see Figure 6,

Preprints.org (www.preprints.org) | NOT PEER-REVIEWED | Posted: 28 April 2026 doi:10.20944/preprints202604.1933.v1

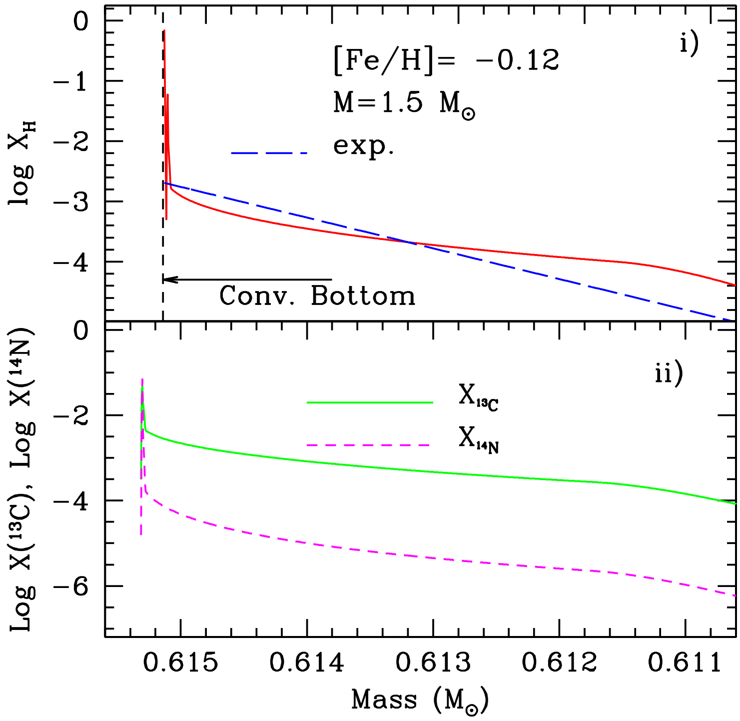

Figure 5. An example of the typical pockets obtained through magnetic buoyancy at TDU, inducing proton penetration with a peculiar pattern (top panel). When H burning restarts, the extended concentration of protons reacts with ^{12}C, producing ^{13}C. There are too few protons to induce the production of any significant amount of ^{14}N, reducing drastically the possible products of its burning, in particular ^{19}F. This clarified its low abundance and its metallicity dependence, previously unexplained [60].

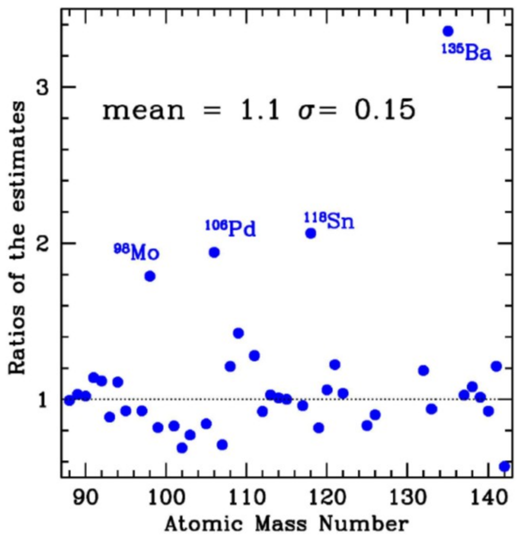

Figure 6. The few remaining discrepancies between the estimates of the *s*-process components at the era of the solar formation, between: i) galactic chemical evolution of TP-AGB products, with magnetically-induced mixing for the *s* process; and ii) estimates of the required (*s* = 1-*r*) fractions, as derived by a model independent approach to the *r* process. (See [61] for details). Some problems do remain on few nuclei (^{135}Ba in particular), but no other attempt ever reached such an agreement on all the other nuclei.

5. The Observational Evidence

A large database has been accumulated in the last thirty years confirming the indication that the right neutron source had been identified. It is not in the scopes of this review to enter into too many details about the observations. We address interested readers to the recent work by Domínguez et al. [62], where this topic is discussed more accurately. We summarize briefly the main points here below.

5.1. Normal AGB Star Observations

Spectroscopic studies of AGB stars have been fundamental in confirming theoretical ideas about internal mixing and neutron capture nucleosynthesis. These stars have extremely complex, crowded spectra, and deriving detailed abundances requires careful modeling of stellar atmospheres. Despite these challenges, hundreds of *s* process element measurements have been obtained over the last decades.

A classical and unambiguous signature of in situ neutron capture is the mentioned detection of technetium (Tc) in AGB star spectra. Since Tc has no stable isotopes and its longest-lived isotopes decay on timescales much shorter than stellar lifetimes, its presence requires recent internal production and dredge up, which are clear markers of active *s* process nucleosynthesis.

Observations of O-rich AGB stars (spectral types MS, S) show enhanced abundances of *s* process elements such as Sr, Y, Zr, Ba, and Nd. These enhancements align well with model predictions in which the $^{13}C(\alpha,n)^{16}$O neutron source operates at relatively low neutron density [45]. Measurements of elements around branch points in the *s* process, in particular rubidium (Rb) relative to other light *s* elements, provide constraints on neutron density and confirm that the dominant neutron source in these stars is ^{13}C, consistent with low mass AGB progenitors . Carbon rich AGB stars (C stars, spectral type N) also show *s* process enhancements at levels comparable to those in S stars, and spectroscopic data demonstrate that these enhancements correlate with decreasing stellar metallicity. Ratios of heavy element abundances such as [hs/ls] (i.e. the relative enhancement of second peak to first peak *s* process elements) increase with decreasing metallicity, as expected if the same amount of neutrons (from ^{13}C) is available for any metal content, so that for a lower abundance of iron seeds the neutrons capture per nucleus increase [63,64]. A wide spread in observed [hs/ls] at each given metallicity indicates variations in the pocket size and hence in the mixing efficiency among different stars.

5.2. Post AGB Stars

Post AGB stars, objects that have left the TP AGB but not yet become white dwarfs, often show significant overabundance of both light and heavy *s*-process elements. Models predict that the *s* process should drive increasingly large lead (Pb) enhancements at lower metallicities, but many observed post AGB stars show upper limits on Pb abundances that are lower than model expectations [65]. Reconciling these discrepancies and matching abundances across the *s* process third peak remains a challenge for current models and may involve revisiting neutron capture paths, branchings, and potential alternative neutron density regimes, such as the intermediate neutron capture process, or *i-process* .

5.3. Pre-Solar Grains

Pre solar grains are microscopic dust particles found in primitive meteorites that retain the isotopic signatures of the stellar winds where they formed. Silicon carbide (SiC) grains thought to originate in C rich AGB star outflows show isotopic enrichments in elements like Sr, Zr, Mo, Ru and Ba that reflect neutron capture conditions in their parent stars [66]. Because these isotopic measurements can be extremely precise, they provide some of the strongest constraints on the extent of the ^{13}C pocket and the mixing processes that formed it. Models that include physical mixing mechanisms (especially MHD induced pocket formation) can reproduce the spread and shapes of isotopic ratios seen in these grains much more faithfully than purely parametric mixing approaches [57].

 doi:10.20944/preprints202604.1933.v1

Acknowledgments: I thank the organizers for their invitation to present this talk and many colleagues (with special emphasis on Sara Palmerini, Diego Vescovi, Sergio Cristallo and Oscar Straniero) for enjoying with me the kind of studies reviewed here for several years. I am grateful to the INFN, section of Perugia, for supporting this visit of mine and for many other forms of kindness, shown especially after my retirement.

References

1. Aston, F.W. The Constitution of the Elements. *Nature* **1919**, *104*, 393. https://doi.org/10.1038/104393b0.
2. Eddington, A.S. The sources of stellar energy. *The Observatory* **1919**, *42*, 371–376.
3. Perrin, J. Matière et lumière. *Annales de Physique* **1919**, *9*, 5–108. https://doi.org/10.1051/anphys/191909110005.
4. Gamow, G. Zur Quantentheorie des Atomkernes. *Zeitschrift fur Physik* **1928**, *51*, 204–212. https://doi.org/10.1007/BF01343196.
5. Atkinson, R.D.E.; Houtermans, F.G. Zur Frage der Aufbaumöglichkeit der Elemente in Sternen. *Zeitschrift fur Physik* **1929**, *54*, 656–665. https://doi.org/10.1007/BF01341595.
6. Atkinson, R.d. Atomic Synthesis and Stellar Energy. III. *ApJ* **1936**, *84*, 73. https://doi.org/10.1086/143750.
7. Bethe, H.A.; Critchfield, C.L. On the Formation of Deuterons by Proton Combination. *Physical Review* **1938**, *54*, 862–862. https://doi.org/10.1103/PhysRev.54.862.2.
8. von Weizsäcker, C.F. Erwiderung zu der Bemerkung von Herrn v. Wisniewski. *Naturwissenschaften* **1939**, *27*, 277–278. https://doi.org/10.1007/BF01495544.
9. Hoyle, F. The synthesis of the elements from hydrogen. *MNRAS* **1946**, *106*, 343. https://doi.org/10.1093/mnras/106.5.343.
10. Hoyle, F. On Nuclear Reactions Occuring in Very Hot STARS.I. the Synthesis of Elements from Carbon to Nickel. *ApJ Suppl. Series* **1954**, *1*, 121. https://doi.org/10.1086/190005.
11. Fewell, M.P. The atomic nuclide with the highest mean binding energy. *American Journal of Physics* **1995**, *63*, 653–658. https://doi.org/10.1119/1.17828.
12. Burbidge, E.M.; Burbidge, G.R.; Fowler, W.A.; Hoyle, F. Synthesis of the Elements in Stars. *Reviews of Modern Physics* **1957**, *29*, 547–650. https://doi.org/10.1103/RevModPhys.29.547.
13. Clayton, D.D.; Fowler, W.A.; Hull, T.E.; Zimmerman, B.A. Neutron capture chains in heavy element synthesis. *Annals of Physics* **1961**, *12*, 331–408. https://doi.org/10.1016/0003-4916(61)90067-7.
14. Clayton, D.D. Chronology of the Galaxy. *Science* **1964**, *143*, 1281–1286. https://doi.org/10.1126/science.143.3612.1281.
15. Seeger, P.A.; Fowler, W.A.; Clayton, D.D. Nucleosynthesis of Heavy Elements by Neutron Capture. *ApJ Suppl. Series* **1965**, *11*, 121. https://doi.org/10.1086/190111.
16. Clayton, D.D. *Principles of stellar evolution and nucleosynthesis*; 1968.
17. Merrill, P.W. Technetium in the stars. *Science* **1952**, *115*, 484. https://doi.org/10.1126/science.115.2992.479.
18. Schwarzschild, M.; Härm, R. Hydrogen Mixing by Helium-Shell Flashes. *ApJ* **1967**, *150*, 961. https://doi.org/10.1086/149396.
19. Clayton, D.D.; Ward, R.A. S-Process Studies: Exact Evaluation of an Exponential Distribution of Exposures. *ApJ* **1974**, *193*, 397–400. https://doi.org/10.1086/153175.
20. Raiteri, C.M.; Gallino, R.; Busso, M.; Neuberger, D.; Kaeppeler, F. The Weak s-Component and Nucleosynthesis in Massive Stars. *NUCLEAR REACTIONS, NUCLEOSYNTHESIS, ABUNDANCES, STARS: EARLY-TYPE, STARS: INTERIORS* **1993**, *419*, 207. https://doi.org/10.1086/173476.
21. Busso, M.; Gallino, R.; Wasserburg, G.J. Nucleosynthesis in Asymptotic Giant Branch Stars: Relevance for Galactic Enrichment and Solar System Formation. *Ann. Rev. Astron.& Astroph.* **1999**, *37*, 239–309. https://doi.org/10.1146/annurev.astro.37.1.239.
22. Ward, R.A.; Newman, M.J. s-process studies: the effect of a pulsed neutron flux. *ApJ* **1978**, *219*, 195–212. https://doi.org/10.1086/155768.
23. Straniero, O.; Abia, C.; Domínguez, I. The carbon star mystery: 40 years later: Theory and observations. *European Physical Journal A* **2023**, *59*, 17, [arXiv:astro-ph.SR/2301.03978]. https://doi.org/10.1140/epja/s10050-023-00926-8.
24. Halabi, G.M. Study of the Thermal Pulsation of AGB Stars. *arXiv e-prints* **2014**, p. arXiv:1410.1682, [arXiv:astro-ph.SR/1410.1682]. https://doi.org/10.48550/arXiv.1410.1682.
25. Straniero, O.; Chieffi, A.; Limongi, M.; Busso, M.; Gallino, R.; Arlandini, C. Evolution and Nucleosynthesis in Low-Mass Asymptotic Giant Branch Stars. I. Formation of Population I Carbon Stars. *ApJ* **1997**, *478*, 332–339. https://doi.org/10.1086/303794.
26. Ulrich, R.K. The s-Process in Stars. In Proceedings of the Explosive Nucleosynthesis; Schramm, D.N.; Arnett, W.D., Eds., 1973, p. 139.
27. Paczyński, B. The Formation of Planetary Nebulae. *Astrophysical Letters* **1971**, *9*, 33.

28. Paczynski, B. Core mass-interflash period relation for double shell source stars. *ApJ* **1975**, *202*, 558–560. https://doi.org/10.1086/154006.
29. Wagenhuber, J.; Groenewegen, M.A.T. New input data for synthetic AGB evolution. *A&A* **1998**, *340*, 183–195, [arXiv:astro-ph/astro-ph/9809338]. https://doi.org/10.48550/arXiv.astro-ph/9809338.
30. Marigo, P. The Initial-Final Mass Relation of White Dwarfs: A Tool to Calibrate the Third Dredge-Up. *Universe* **2022**, *8*, 243, [arXiv:astro-ph.SR/2204.06470]. https://doi.org/10.3390/universe8040243.
31. Marigo, P.; Bossini, D.; Trabucchi, M.; Addari, F.; Girardi, L.; Cummings, J.D.; Pastorelli, G.; Dal Tio, P.; Costa, G.; Bressan, A. A Fresh Look at AGB Stars in Galactic Open Clusters with Gaia: Impact on Stellar Models and the Initial-Final Mass Relation. *ApJ Suppl. Series* **2022**, *258*, 43, [arXiv:astro-ph.SR/2111.03527]. https://doi.org/10.3847/1538-4365/ac374a.
32. Iben, Jr., I. Thermal pulses: p-capture, alpha -capture, s-process nucleosynthesis; and convective mixing in a star of intermediate mass. *ApJ* **1975**, *196*, 525–547. https://doi.org/10.1086/153433.
33. Truran, J.W.; Iben, Jr., I. On s-process nucleosynthesis in thermally pulsing stars. *ApJ* **1977**, *216*, 797–810. https://doi.org/10.1086/155523.
34. Iben, Jr., I.; Truran, J.W. On the surface composition of thermally pulsing stars of high luminosity and on the contribution of such stars to the element enrichment of the interstellar medium. *ApJ* **1978**, *220*, 980–995. https://doi.org/10.1086/155986.
35. Becker, S.A.; Iben, Jr., I. The asympiotic giant branch evolution of intermediate-mass stars as a function of mass and composition. II. Through the first major thermal pulse and the consequences of convective dredge-up. *ApJ* **1980**, *237*, 111–129. https://doi.org/10.1086/157850.
36. Smith, V.V.; Lambert, D.L. The chemical composition of red giants. I. Dredge-up in the M and MS stars. *ApJ* **1985**, *294*, 326–338. https://doi.org/10.1086/163300.
37. Smith, V.V.; Lambert, D.L. The Chemical Composition of Red Giants. II. Helium Burning and the s-Process in the MS and S Stars. *ApJ* **1986**, *311*, 843. https://doi.org/10.1086/164823.
38. Smith, V.V.; Lambert, D.L. The Chemical Composition of Red Giants. III. Further CNO Isotopic and s-Process Abundances in Thermally Pulsing Asymptotic Giant Branch Stars. *ApJ Suppl. Series* **1990**, *72*, 387. https://doi.org/10.1086/191421.
39. Iben, Jr., I. On intermediate-mass single stars and accreting white dwarfs as sources of neutron-rich isotopes. *ApJ* **1981**, *243*, 987–993. https://doi.org/10.1086/158663.
40. Iben, Jr., I.; Renzini, A. On the formation of carbon star characteristics and the production of neutron-rich isotopes in asymptotic giant branch stars of small core mass. *ApJL* **1982**, *263*, L23–L27. https://doi.org/10.1086/183916.
41. Gilroy, K.K. Carbon Isotope Ratios and Lithium Abundances in Open Cluster Giants. PhD thesis, University of Texas, Austin, 1988.
42. Gilroy, K.K. More About $^{12}C/^{13}C$ Ratios in Cluster Giants &Subgiants. In Proceedings of the Bulletin of the American Astronomical Society, 1989, Vol. 21, p. 790.
43. Gilroy, K.K.; Brown, J.A. Carbon Isotope Ratios along the Giant Branch of M67. *ApJ* **1991**, *371*, 578. https://doi.org/10.1086/169922.
44. Gustafsson, B. Towards a Satisfactory Understanding of AGB-Star Atmospheres? In Proceedings of the Why Galaxies Care About AGB Stars: Their Importance as Actors and Probes; Kerschbaum, F.; Charbonnel, C.; Wing, R.F., Eds., 2007, Vol. 378, *Astronomical Society of the Pacific Conference Series*, p. 60.
45. Lambert, D.L.; Smith, V.V.; Busso, M.; Gallino, R.; Straniero, O. The Chemical Composition of Red Giants. IV. The Neutron Density at the s-Process Site. *ApJ* **1995**, *450*, 302. https://doi.org/10.1086/176141.
46. Busso, M.; Picchio, G.; Gallino, R.; Chieffi, A. Are s-Elements Really Produced during Thermal Pulses in Intermediate-Mass Stars? *ApJ* **1988**, *326*, 196. https://doi.org/10.1086/166081.
47. Gallino, R.; Busso, M.; Picchio, G.; Raiteri, C.M.; Renzini, A. On the Role of Low-Mass Asymptotic Giant Branch Stars in Producing a Solar System Distribution of s-Process Isotopes. *ApJL* **1988**, *334*, L45. https://doi.org/10.1086/185309.
48. Kaeppeler, F.; Gallino, R.; Busso, M.; Picchio, G.; Raiteri, C.M. S-Process Nucleosynthesis: Classical Approach and Asymptotic Giant Branch Models for Low-Mass Stars. *ApJ* **1990**, *354*, 630. https://doi.org/10.1086/168720.
49. Straniero, O.; Gallino, R.; Busso, M.; Chiefei, A.; Raiteri, C.M.; Limongi, M.; Salaris, M. Radiative 13C Burning in Asymptotic Giant Branch Stars and s-Processing. *ApJL* **1995**, *440*, L85. https://doi.org/10.1086/187767.
50. Gallino, R.; Arlandini, C.; Busso, M.; Lugaro, M.; Travaglio, C.; Straniero, O.; Chieffi, A.; Limongi, M. Evolution and Nucleosynthesis in Low-Mass Asymptotic Giant Branch Stars. II. Neutron Capture and the S-Process. *ApJ* **1998**, *497*, 388–403. https://doi.org/10.1086/305437.

51. Nucci, M.C.; Busso, M. Magnetohydrodynamics and Deep Mixing in Evolved Stars. I. Two- and Three-dimensional Analytical Models for the Asymptotic Giant Branch. *ApJ* **2014**, *787*, 141, [arXiv:astro-ph.SR/1404.2503]. https://doi.org/10.1088/0004-637X/787/2/141.
52. Denissenkov, P.A.; Tout, C.A. Partial mixing and formation of the ^{13}C pocket by internal gravity waves in asymptotic giant branch stars. *MNRAS* **2003**, *340*, 722–732. https://doi.org/10.1046/j.1365-8711.2003.06284.x.
53. Battino, U.; Lederer-Woods, C.; Cseh, B.; Denissenkov, P.; Herwig, F. Mixing Uncertainties in Low-Metallicity AGB Stars: The Impact on Stellar Structure and Nucleosynthesis. *Universe* **2021**, *7*, 25. https://doi.org/10.3390/universe7020025.
54. Trippella, O.; Busso, M.; Palmerini, S.; Maiorca, E.; Nucci, M.C. s-Processing in AGB Stars Revisited. II. Enhanced 13C Production through MHD-induced Mixing. *ApJ* **2016**, *818*, 125, [arXiv:astro-ph.SR/1512.06777]. https://doi.org/10.3847/0004-637X/818/2/125.
55. Vescovi, D.; Cristallo, S. Modeling the formation of the ^{13}C neutron source in AGB stars. In Proceedings of the Journal of Physics Conference Series. IOP, 2020, Vol. 1668, *Journal of Physics Conference Series*, p. 012047, [arXiv:astro-ph.SR/2004.01645]. https://doi.org/10.1088/1742-6596/1668/1/012047.
56. Busso, M.; Vescovi, D.; Palmerini, S.; Cristallo, S.; Antonuccio-Delogu, V. s-processing in AGB Stars Revisited. III. Neutron Captures from MHD Mixing at Different Metallicities and Observational Constraints. *ApJ* **2021**, *908*, 55, [arXiv:astro-ph.SR/2011.07469]. https://doi.org/10.3847/1538-4357/abca8e.
57. Palmerini, S.; Busso, M.; Vescovi, D.; Naselli, E.; Pidatella, A.; Mucciola, R.; Cristallo, S.; Mascali, D.; Mengoni, A.; Simonucci, S.; et al. Presolar Grain Isotopic Ratios as Constraints to Nuclear and Stellar Parameters of Asymptotic Giant Branch Star Nucleosynthesis. *ApJ* **2021**, *921*, 7, [arXiv:astro-ph.SR/2107.12037]. https://doi.org/10.3847/1538-4357/ac1786.
58. Vescovi, D.; Cristallo, S.; Palmerini, S.; Abia, C.; Busso, M. Magnetic-buoyancy-induced mixing in AGB stars: Fluorine nucleosynthesis at different metallicities. *A&A* **2021**, *652*, A100, [arXiv:astro-ph.SR/2106.08241]. https://doi.org/10.1051/0004-6361/202141173.
59. Busso, M.M.; Kratz, K.L.; Palmerini, S.; Akram, W.; Antonuccio-Delogu, V. Production of solar abundances for nuclei beyond Sr: The s- and r-process perspectives. *Frontiers in Astronomy and Space Sciences* **2022**, *9*, 956633. https://doi.org/10.3389/fspas.2022.956633.
60. Vescovi, D.; Cristallo, S.; Palmerini, S.; Abia, C.; Busso, M. Magnetic-buoyancy-induced mixing in AGB stars: Fluorine nucleosynthesis at different metallicities. *A&A* **2021**, *652*, A100, [arXiv:astro-ph.SR/2106.08241]. https://doi.org/10.1051/0004-6361/202141173.
61. Busso, M.M.; Kratz, K.L.; Palmerini, S.; Akram, W.; Antonuccio-Delogu, V. Production of solar abundances for nuclei beyond Sr: The s- and r-process perspectives. *Frontiers in Astronomy and Space Sciences* **2022**, *9*, 956633. https://doi.org/10.3389/fspas.2022.956633.
62. Domínguez, I.; Abia, C.; Busso, M.; Palmerini, S.; Straniero, O. s-process nucleosynthesis in low-mass AGB stars by the 13C(α,n)16O neutron source. *European Physical Journal A* **2026**, *62*, 53, [arXiv:astro-ph.SR/2603.08140]. https://doi.org/10.1140/epja/s10050-026-01810-x.
63. Abia, C.; Wallerstein, G. Heavy-element abundances in seven SC stars and several related stars. *MNRAS* **1998**, *293*, 89–106. https://doi.org/10.1046/j.1365-8711.1998.01157.x.
64. Abia, C.; de Laverny, P.; Cristallo, S.; Kordopatis, G.; Straniero, O. Properties of carbon stars in the solar neighbourhood based on Gaia DR2 astrometry. *A&A* **2020**, *633*, A135, [arXiv:astro-ph.SR/1911.09413]. https://doi.org/10.1051/0004-6361/201936831.
65. De Smedt, K.; Van Winckel, H.; Kamath, D.; Siess, L.; Goriely, S.; Karakas, A.I.; Manick, R. Detailed homogeneous abundance studies of 14 Galactic s-process enriched post-AGB stars: In search of lead (Pb). *A&A* **2016**, *587*, A6, [arXiv:astro-ph.SR/1512.05393]. https://doi.org/10.1051/0004-6361/201527430.
66. Liu, N.; Savina, M.R.; Gallino, R.; Davis, A.M.; Bisterzo, S.; Gyngard, F.; Käppeler, F.; Cristallo, S.; Dauphas, N.; Pellin, M.J.; et al. Correlated Strontium and Barium Isotopic Compositions of Acid-cleaned Single Mainstream Silicon Carbides from Murchison. *ApJ* **2015**, *803*, 12, [arXiv:astro-ph.SR/1501.05883]. https://doi.org/10.1088/0004-637X/803/1/12.